

A Portable 16-Channel Magnetic Sensor For Human Magnetocardiographic Experiments

Young Jin Kim¹, Igor Savukov²

^{1,2}P-21 Applied Modern Physics Group, Los Alamos National Laboratory, PO Box 1663, MS-D454, Los Alamos, NM 87545, USA

Corresponding Author: Young Jin Kim

Abstract: We constructed a portable, low-cost 16-channel magnetic sensor for magnetocardiography (MCG) applications. The sensor is based on a high-sensitivity optically pumped magnetometer (OPM) with a novel configuration of nearly parallel pump and probe laser beams. The OPM-based 16-channel magnetic sensing is realized in a single module by using a fairly large rubidium vapor cell, broad pump/probe laser beams, and a 16-channel photodiode array, leading projected 10-fold reduction of the cost of sensors. The portability of the sensor is achieved by coupling the pump and probe lasers to OPM optics through multi-mode optical fibers. The 16-channel magnetic sensor is surrounded by a non-magnetic enclosure for safe operation. For MCG experiments with the sensor, its main components except lasers are located inside a magnetically shielded room (MSR), which reduces the ambient magnetic noise. The location of lasers and supporting electronics outside the MSR improves the sensitivity of the sensor. We report that the 16-channel magnetic sensor has a magnetic field sensitivity sufficient to directly detect the human cardiac magnetic signals.

Keywords – Optically pumped magnetometer; Magnetocardiography; 16-channel magnetic sensing; Portability; Magnetically shield room

Date of Submission: 05-10-2018

Date of acceptance: 17-10-2018

I. Introduction

Magnetocardiography (MCG) is a noninvasive technique to image the heart's electrical activity by detecting the magnetic fields at the chest location. Since the first MCG measurement based on coils as a magnetic sensor in 1963 [1], MCG experiments have been continuously improved, in particular with the development of state-of-the-art superconducting quantum interference device (SQUID) magnetometers that drastically enhanced the sensitivity to the heart magnetic signals [2]. SQUID-based MCG devices operated inside magnetically shield rooms (MSRs) reached a comparable sensitivity as electrocardiography (ECG), the widely spread technology for studying the heart's electrical activity by detecting the electrical potentials with electrodes attached to the skin on the chest. This has attracted wide interest of the biomagnetism community to MCG. Recently, MCG was found to be a more accurate and in some cases more convenient (avoiding direct contact with the skin that can be damaged) diagnostic method than ECG [3]. Other advantages could be the absence of the artifacts due to conductivity non-uniformity.

Despite of high-sensitivity of SQUID-based magnetic sensors, they have a major problem of high cost due to liquid helium cooling, approximately \$250k per year. Hence, new inventions in magnetic sensors are still needed to improve the MCG technology and make it widely deployable in clinics. One promising approach is to replace SQUIDS with optically pumped magnetometers (OPMs), which are the most sensitive room-temperature magnetic-field sensors with sensitivity similar to that of SQUIDS. In addition, multichannel parallel magnetic imaging is required to accelerate magnetic imaging of the heart at the same time [4-5]. One quick method to build an OPM-based multichannel magnetic sensor is to combine the best commercially available single-channel OPMs produced by QuSpin Inc. [6] into an array. Although they can reach the sensitivity of ~ 10 fT/Hz^{1/2} [6], the price of each OPM is around \$10k and the construction of 16 sensing channels can cost around \$160k, still quite high.

In this letter, we present a promising OPM-based 16-channel magnetic sensor in a single module enabling applications in MCG, as well as in other fields requiring sensitive magnetic imaging. This system utilizes a single large alkali-metal vapor cell and broad laser beams to realize 16 sensing channels. Compared to a magnetic sensor composed of 16 individual commercial QuSpin OPMs, our single-module 16-channel magnetic sensor can reduce the sensor cost by an order of magnitude and minimize the fabrication effort. Our sensor is also easy to relocate by using an original flexible design based on coupling lasers to fibers. This sensor is fully surrounded by a non-magnetic wooden enclosure to make MCG experiments safe for human subjects inside an MSR.

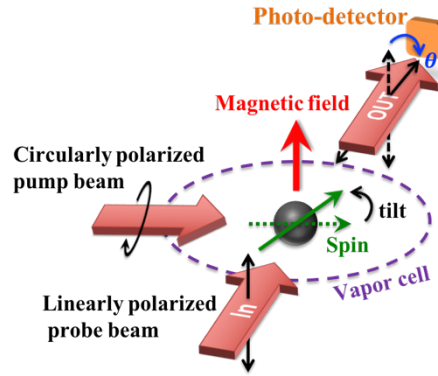


Figure 1: OPM configuration. Two laser beams are used: a pump beam to polarize atomic spins and a probe beam to read out the state of the spins.

II. Design of 16-channel magnetic sensor

The basic principle of the OPMs used in our 16-channel magnetic sensor is shown in Fig. 1. Two laser beams for pumping and probing are sent to overlap in a rubidium (Rb) vapor cell. Note that the best sensitivity is expected in case of orthogonal beams which have wavelengths individually optimized, but other beam configurations are used, and in the experiments described here we employed the near parallel beam configuration; the orthogonal beam configuration is also useful for the purpose of explaining the OPM principles. A circularly polarized pump laser beam orients Rb electron spins along its direction. This action creates a large number of 100% polarized electron spins in the vapor cell. The interaction between a weak external magnetic field and the polarized spins tilts the spin orientation by a small angle, proportional to the field magnitude. The tilt angle (thus the magnetic field) is measured by the effect of the spins on the polarization plane rotation of a linearly polarized probe laser beam (Faraday effect), using a polarimeter containing a photo-detector. The orthogonal beam configuration provides very high magnetic field sensitivity of $1 \text{ fT/Hz}^{1/2}$ [7], but in the limited shielding environment, such configuration might not be essential. Lately, the parallel beam configuration has become popular due to simplifications that it offers. It was recently demonstrated that an OPM with parallel beams can reach a $10 \text{ fT/Hz}^{1/2}$ sensitivity at low frequency below 100 Hz [8]. The OPMs with such sensitivity have been used for precision experiments, magnetoencephalography (MEG), and other ultra-sensitive bioimaging.

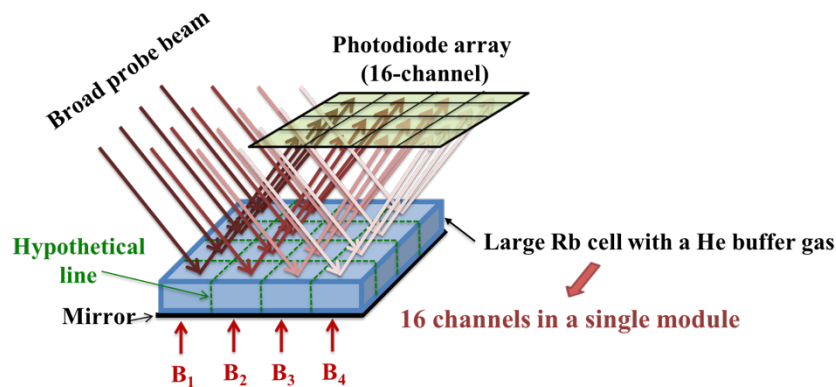


Figure 2: Illustration of 16-channel magnetic sensing in a single module based on a single large Rb vapor cell, broad laser beam, and 16-channel photodiode array.

Figure 2 shows the concept of the novel approach of a 16-channel magnetic sensor based on OPM. The important feature of this approach is implementation of 16 sensing channels in a single module. This is achieved based on a single large Rb vapor cell filled with about 1 amagat of helium buffer gas, broad laser beams for pumping and probing, and a 4 by 4 photodiode array. The buffer gas in the cell is added to restrain the motion of Rb atoms, resulting in multiple individual local field sensing volumes in the cell. Thus, the large cell converts magnetic images to optical images with a broad probe beam. The optical images are read out with the photodiode array. The reflection of laser beams (pump beam is not shown in Fig. 2) by a mirror located at the bottom of the cell minimizes the stand-off distance to human subjects and doubles the magnetic signals [8].

To test the feasibility of this approach, we have built a prototype of 16-channel magnetic sensor and experimentally demonstrated high sensitivity of a few tens femto-Tesla in each channel of the prototype [9]. For future MCG experiments we redesigned the 16-channel prototype sensor using only non-magnetic materials and completely surrounded it by a wooden enclosure as shown in Fig. 3(a). The probe and pump lasers, coupled to optics through multi-mode fibers, are also fully enclosed by a plastic case (the photograph shown below). The power of lasers is about 30 mW (Class 3B lasers), hazardous for eye exposure. However, the wooden enclosure makes the sensor a Class 1 laser system, which will make MCG experiments safe for human subjects inside an MSR. Figure 3(b) shows a Rb vapor cell of flat pancake shape with 6 cm diameter and 2 cm thickness. The cell requires to be heated to about 160°C to acquire a high number density of Rb atoms and to operate the magnetometer in the spin-exchange relaxation-free (SERF) regime [8]. For this, the Rb cell is surrounded by microporous heat insulation with 1 cm thickness. The cell window is left open to allow probe and pump laser beams to enter the cell. To remove residual dc magnetic fields and magnetic gradients at the location of the cell inside the MSR, a compensation coil system is added around the cell as shown in Fig. 3(a). The coil system is composed of three orthogonal coils and three gradient coils (dB_x/dx , dB_y/dy , and dB_z/dz). The 4 by 4 photodiode array is mounted on an aluminum box with 16 cables which are connected to a data acquisition system through a 16-channel transimpedance amplifier. More details on the sensor's configuration can be found in Ref. [9].

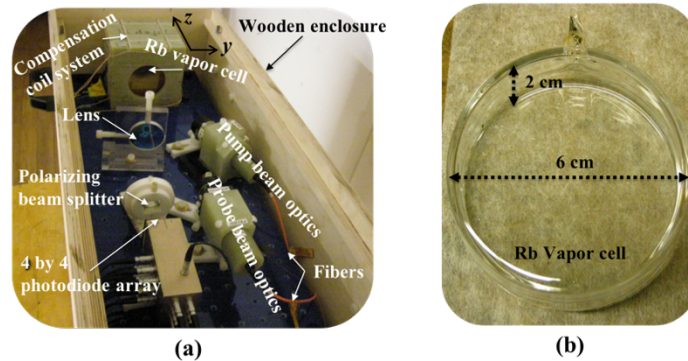
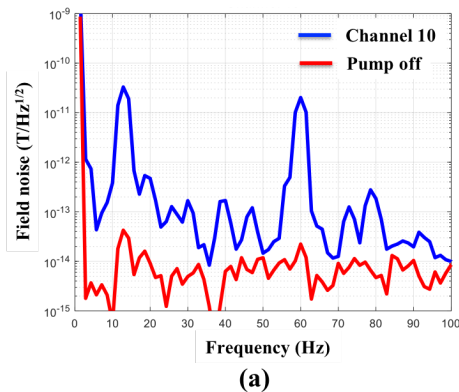


Figure 3: Photograph of (a) the 16-channel magnetic sensor inside a wooden enclosure (a wooden lid is removed for illustration purpose only) and (b) the Rb vapor cell

III. Performance Evaluation

We evaluated the performance of our enclosed 16-channel magnetic sensor inside an one-layer open μ -metal shield with 50 cm diameter and 101 cm length. The magnetic field sensitivity in the y direction [see Fig. 3(a)] was investigated. An oscillating calibration magnetic field of 33 pT at 13 Hz was applied in the y direction using the B_y coil (also used for compensation of residual B_y in the shield) in order to convert the recorded voltage noise of the photodiode array into the magnetic field noise.



Ch. 1 74 fT/Hz ^{1/2}	Ch. 2 71 fT/Hz ^{1/2}	Ch. 3 64 fT/Hz ^{1/2}	Ch. 4 84 fT/Hz ^{1/2}
Ch. 5 108 fT/Hz ^{1/2}	Ch. 6 54 fT/Hz ^{1/2}	Ch. 7 53 fT/Hz ^{1/2}	Ch. 8 162 fT/Hz ^{1/2}
Ch. 9 87 fT/Hz ^{1/2}	Ch. 10 53 fT/Hz ^{1/2}	Ch. 11 43 fT/Hz ^{1/2}	Ch. 12 79 fT/Hz ^{1/2}
Ch. 13 83 fT/Hz ^{1/2}	Ch. 14 81 fT/Hz ^{1/2}	Ch. 15 53 fT/Hz ^{1/2}	Ch. 16 104 fT/Hz ^{1/2}

Figure 4: (a) Magnetic field noise spectrum of channel 10 of the 16-channel magnetic sensor. (b) Magnetic field sensitivities of all 16 sensing channels of the sensor.

Figure 4(a) shows the measured magnetic field noise spectrum of channel 10 of the 16-channel magnetic sensor as an example. The blue curve indicates the field sensitivity of about 50 fT/Hz^{1/2} at low frequency in the partially shielded area. The peaks at 13 Hz and 60 Hz are from the calibration field and 60 Hz

building power, respectively. The red curve shows the intrinsic OPM sensitivity, which is limited by the probe beam noise, when the pump beam was shut off. The intrinsic sensitivity reaches to a few $\text{fT}/\text{Hz}^{1/2}$; therefore, the field sensitivity of the sensor can be improved to a few femto-Tesla with a better shielding, which can be achieved inside an MSR. Figure 4(b) shows magnetic field sensitivities in all 16 sensing channels. Intensity non-uniformity of the broad laser beams is the main reason for the large discrepancy of the sensitivities. Several measures in the future can be implemented to improve the uniformity, such as the use of single-mode fibers and higher laser power that would allow to select a more uniform intensity distribution within the Gaussian profile. However, even the current sensitivity is already sufficient to carry out MCG experiments inside an MSR.

We set up the enclosed 16-channel magnetic sensor inside a two-layer MSR as shown in Fig. 5(a). The residual field inside the MSR was at the nano-Tesla level. The Rb cell was located near the end of the wooden enclosure [left in Fig. 5(a)] to detect the heart magnetic signal in future MCG experiments. The stand-off distance to the chest of a human subject is around 1.5 cm. The currents for the compensation fields are applied to the vapor cell through BNC cables connected to a 8-channel 16-bit waveform analog output, located outside the MSR as shown in Fig. 5 (b). The lasers are also completely enclosed in a plastic case and only fibers pass through the port of the MSR wall [Fig. 5 (a)]. In the near future, we will conduct MCG experiments with this 16-channel magnetic sensor.

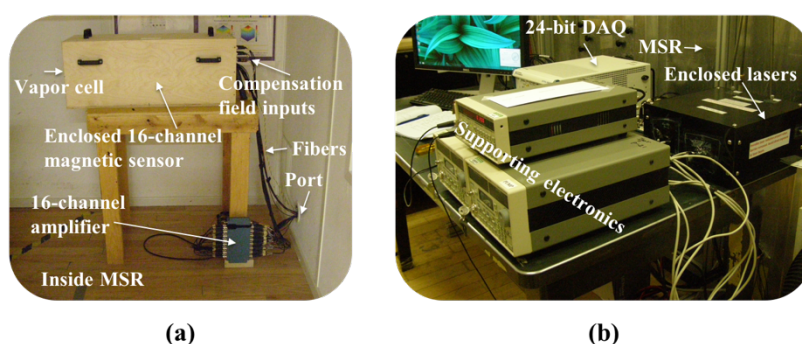


Figure 5: (a) The 16-channel magnetic sensor located inside the MSR. (b) The enclosed lasers and supporting electronics located outside the MSR. The lasers are coupled to optics inside the wooden enclosure through fibers.

IV. Conclusion

For anticipated MCG applications, we have constructed a 16-channel portable and inexpensive OPM sensor using non-magnetic materials. It is based on a single large Rb vapor cell with buffer gas to realize multiple independent sensing channels. The pump and probe laser beams were arranged in the near-parallel beam configuration. Multi-mode optical fibers were used to allow flexibility in the positioning of the sensor. To make MCG experiments safe for human subjects, the sensor and the lasers have been entirely surrounded by enclosures made of wood and plastic. We experimentally investigated the performance of the sensor in a one-layer mu-metal shield and demonstrated that it has sufficient magnetic-field sensitivity for MCG experiments. For MCG experiments inside an MSR, we positioned the lasers and electronics that can generate significant magnetic noise outside, while the 16-channel magnetic sensor that contains the Rb cell and optics inside. In the near future, the sensor in this arrangement will be applied to directly detect the magnetic field from a human heart inside the MSR.

Further sensitivity enhancement of the sensor by increasing intensity and uniformity of laser beams will enable the application of the sensor to MEG or magnetic resonance imaging, both of which requires a few femto-Tesla sensitivity.

Acknowledgements

This work was supported by the U. S. DOE through the Los Alamos National Laboratory LDRD program. The authors are grateful for the helpful assistance of Shaun Newman.

References

- [1]. G. M. Baule and R. McFee, Detection of the magnetic field of the heart, *Am. Heart J.*, 66, 1963, 95-96
- [2]. G. Hart, Biomagnetometry: imaging the heart's magnetic field, *Br. Heart J.*, 65, 1991, 61-62
- [3]. F. E. Smith, P. Langley, P. Leeuwen, B. Hailer, L. Trahms, U. Steinhoff, J. P. Bourke, A. Murray, Comparison of magnetocardiography and electrocardiography: a study of automatic measurement of dispersion of ventricular repolarization, *EP Europace*, 8, 2006, 887-893

- [4]. G. Bison. et al., A room temperature 19-channel magnetic field mapping device for cardiac signals, *Appl. Phys. Lett.*, 95, 2009, 173701
- [5]. Y. H. Lee et al., Multichannel MCG systems with Optimum Combinations of Pickup Coils and Shielded Rooms, 2007 Joint Meeting of the 6th International Symposium on Noninvasive Functional Source Imaging of the Brain and Heart and the International Conference on Functional Biomedical Imaging, Hangzhou, 2007, 297-300
- [6]. QuSpin. Inc. Available at: <http://www.quspin.com>
- [7]. J. C. Allred, R. N. Lyman, T. W. Kornack and M. V. Romalis, High-sensitivity atomic magnetometer unaffected by spin-exchange relaxation, *Phys. Rev. Lett.*, 89, 2002, 130801
- [8]. T. Karaulanov, I. Savukov and Y. J. Kim, Spin-exchange relaxation-free magnetometer with nearly parallel pump and probe beams, *Meas. Sci. Technol.*, 27, 2016, 055002
- [9]. Y. J. Kim and I. Savukov, Highly Sensitive Multi-Channel Atomic Magnetometer, *IEEE Sens. Appl. Symp.*, 1-4, 2018.

Young Jin Kim "A Portable 16-Channel Magnetic Sensor For Human Magnetocardiographic Experiments "International Journal of Engineering Science Invention (IJESI), vol. 07, no. 10, 2018, pp 54-57